

High-mass star-forming cloud G0.38+0.04 in the Galactic center dust ridge contains H₂CO and SiO masers

Adam Ginsburg¹, Andrew Walsh², Christian Henkel^{3, 4}, Paul A. Jones⁵, Maria Cunningham⁵, Jens Kauffmann³, Thushara Pillai³, Elisabeth A.C. Mills⁷, Juergen Ott⁷, J.M. Diederik Kruijssen⁸, Karl M. Menten³, Cara Battersby⁹, Jill Rathborne⁶, Yanett Contreras¹⁰, Steven Longmore¹¹, Daniel Walker¹¹, Joanne Dawson^{6, 12}, John A.P. Lopez⁵

(Affiliations can be found after the references)

2022/05/28

ABSTRACT

We have discovered a new H₂CO (formaldehyde) 1_{1,0} – 1_{1,1} 4.82966 GHz maser in Galactic center Cloud C, G0.38+0.04. At the time of acceptance, this is the eighth region to contain an H₂CO maser detected in the Galaxy. Cloud C is one of only two sites of confirmed high-mass star formation along the Galactic center ridge, affirming that H₂CO masers are exclusively associated with high-mass star formation. This discovery led us to search for other masers, among which we found new SiO vibrationally excited masers, making this the fourth star-forming region in the Galaxy to exhibit SiO maser emission. Cloud C is also a known source of CH₃OH Class-II and OH maser emission. There are now two known regions that contain both SiO and H₂CO masers in the CMZ, compared to two SiO and six H₂CO in the Galactic disk, while there is a relative dearth of H₂O and CH₃OH Class-II masers in the CMZ. SiO and H₂CO masers may be preferentially excited in the CMZ, perhaps because of higher gas-phase abundances from grain destruction and heating, or alternatively H₂O and CH₃OH maser formation may be suppressed in the CMZ. In any case, Cloud C is a new testing ground for understanding maser excitation conditions.

Key words. Masers Radio lines: ISM Galaxy: center ISM: clouds ISM: molecules ISM:individual objects: Cloud C

1. Introduction

Masers are important tracers of star formation, shocked gas, evolved stars, and in other galaxies, circumnuclear disks. While many masers are common in the Galaxy and readily detected in other galaxies (e.g., OH, CH₃OH, and H₂O), H₂CO has only been detected as a maser in seven locations within our Galaxy, and so far no instances have been confirmed in other galaxies (Araya et al. 2007a; Mangum et al. 2008)¹.

Most of the H₂CO masers detected so far have been observed as part of dedicated surveys targeting high-mass young stellar objects (YSOs; Araya et al. 2004, 2007b, 2008). Despite concerted effort, very few new masers outside of Sgr B2 (Whiteoak et al. 1983; Mehringer et al. 1994) have been found since their initial discovery by Forster et al. (1980). All of the known H₂CO masers are associated with regions of high-mass star formation (Pratap et al. 1994; Araya et al. 2004, 2007b, 2008).

The pumping mechanism of the H₂CO 1_{1,0} – 1_{1,1} maser is not yet understood. A radio continuum pumping mechanism was proposed by Boland & de Jong (1981) and later van der Walt (2014), but the lack of bright radio continuum sources near some of the detected H₂CO maser sources

means that this mechanism cannot explain all of the observed masers (Mehringer et al. 1994; Araya et al. 2008). van der Walt (2014) ruled out infrared pumping, but suggest that collisional pumping may be a viable mechanism. In the van der Walt (2014) framework, high amplifications > 20 are not possible, so additional physical mechanisms must be in play for the brightest H₂CO masers.

SiO masers are common toward oxygen-rich evolved stars, namely long period variables (Mira stars) and red supergiants (see, e.g., Deguchi et al. 2004; Verheyen et al. 2012), but extremely rare toward star-forming regions, with only three known (Zapata et al. 2009b). In the few regions where they have been detected - W51 North, Sgr B2 (M), and Orion KL - they closely trace the location of the high-mass YSO, likely pinpointing the base of a high-velocity outflow (Goddi et al. 2015).

Cloud C, G0.38+0.04, is one of the high-column-density clouds along the central molecular zone (CMZ) dust ridge (Lis et al. 1999; Immer et al. 2012). It is notable for containing the brightest 70 μm point source along that ridge and the third brightest (after Sgr B2 and Sgr C) along the Kruijssen et al. (2015) orbit (Molinari et al. 2011). It is not detected at 8 μm with Spitzer (Yusef-Zadeh et al. 2009) and is therefore unlikely to be an evolved star, but it is associated with extended 4.5 μm emission that is generally observed to be associated with molecular (H₂) outflows (Chambers et al. 2011). It is among the most centrally condensed millimeter sources in the CMZ. With a mass in the range 150-2000 M_⊙, depending on the assumed tempera-

¹ Baan et al. (1986) claimed a maser detection in Arp 220, but Mangum et al. (2008) reported that this emission can be explained by thermal processes. However, Baan (private communication) reports that high-resolution observations reveal the emission to be nonthermal. The debate seems unresolved at present.

ture, it may contain a single proto-O-star or a proto-cluster (from the SMA-CMZ survey; Battersby, Keto, et al in prep, Walker et al. in prep).

In the following Letter, we present the serendipitous detection of a H₂CO maser and corresponding new detections of SiO masers in G0.38+0.04.

2. Observations

ATCA observations were performed in 2015 as part of a larger survey of the CMZ. Observations were conducted on April 2 and 13, May 11, August 12 and 13, and September 1 and 4 in the H214, 6A, 1.5C, H75, H75, EW352, and 750B arrays, respectively. The same spectral setup was used for each array configuration, which included observations of 14 spectral lines between approximately 4 and 8 GHz. One of our main target lines is the $1_{1,0} - 1_{1,1}$ transition of H₂CO at 4.82966 GHz. The zoom window at the H₂CO frequency yields a channel resolution of 1.9 km s⁻¹ over a velocity range 3969 km s⁻¹. The sensitivity of the observations was $\sigma = 2$ mJy/beam in each 1.9 km s⁻¹ channel. We assume in this paper that the absolute positional uncertainty of the observations is typically 0.4'' but no worse than 1.0'', based on previous ATCA observations (Caswell 2009).

3. Analysis

We detect spatially and spectrally unresolved H₂CO $1_{1,0} - 1_{1,1}$ emission in one narrow line ($\sigma < 1.3$ km s⁻¹, below the instrument resolution) at $v = 36.7$ km s⁻¹ with an amplitude of 235 mJy/beam, where the restoring beam is 4.84'' × 1.49''. This translates to a brightness temperature of 1700 K. Molecular emission lines with this brightness are generally, not observed in thermally excited regions, so it indicates that there is maser emission.

Since the source is spatially and spectrally unresolved, this brightness temperature is a lower limit. If the true emitting area is 200 au, such as in the Hoffman et al. (2007) Sgr B2 maser spots, the true surface brightness is $T_B = 10^{7.4}$ K. If the line is narrower than our upper limit of $\sigma < 1.3$ km s⁻¹, it may be even brighter.

A literature search revealed that both a Class-II CH₃OH $5_1 - 6_0$ A⁺ (6.67 GHz) maser and H₂O and OH masers have been detected toward Cloud C (Caswell 1998; Argon et al. 2000; Pestalozzi et al. 2005; Caswell 2009; Caswell et al. 2010; Walsh et al. 2011, 2014). We have measured the position of the 6.67 GHz CH₃OH maser from our own data, and it coincides with the H₂CO maser in position to well within the statistical fit errors, much less than the absolute positional uncertainty ($< 0.1''$). There is a water maser within 1 km s⁻¹ of the H₂CO line, and the brightest water maser is separated by only 4 km s⁻¹, so these may arise from the same region; these H₂O masers are coincident with the H₂CO masers to within the systematic pointing errors. The OH and CH₃OH masers are also within about 1 km s⁻¹ of the H₂CO line.

We searched the Jones et al. (2013) Mopra 7mm survey of the Class I CH₃OH $7_0 - 6_1$ A⁺ (44.069476 GHz) line for emission and found a weak, spatially unresolved line with peak brightness 0.06 K (0.5 Jy) at the position and velocity of the H₂CO maser. Assuming the emission comes from $< 1''$ on the sky, as is observed in the H₂CO line, the true brightness must be > 300 K, which suggests that this transition is masing. However, Chambers et al. (2011) observed

this transition with the EVLA and reported a nondetection with a sensitivity of 70 mJy/beam, so further investigation of this line is warranted.

We also searched the Jones et al. (2013) data for the SiO $v=1$ and $v=2$ J=1-0 lines (43.122079 and 42.820582 GHz). We have clearly detected spatially unresolved emission in both lines at ~ 64 km s⁻¹ at the position of Cloud C. The detection of vibrationally excited SiO is a strong indication that these are indeed masing transitions. Figure 1 shows that there is a position offset between the Mopra-detected SiO and CH₃OH 44 GHz masers and the ATCA-detected masers. This is most likely because the centroid errors from the fit to the Mopra moment-0 images are underestimated; there are systematic errors in the Mopra maps ('streaking' artifacts) that affect sub-resolution centroiding.

The SiO masers are offset by $\sim 15 - 20$ km s⁻¹ from most of the other lines, but their velocities lie within the full range of the H₂O masers. This difference suggests that the H₂CO and CH₃OH and some of the H₂O maser points trace a central protostellar core or disk, while the high-velocity H₂O and SiO lines may trace part of an outflow or some other structure.

Finally, we searched the Jones et al. (2012) Mopra 3mm survey for SiO $v=1$ J=2-1 86.243 GHz emission, but did not detect any, with a $3 - \sigma$ upper limit of 96 mK or 0.89 Jy. Given the detection of the 1-0 line at 0.56 Jy, this non-detection is not surprising.

The spectral resolution of the Mopra data is 3.6 km s⁻¹, which is close to the FWHM of the measured lines. Given the limited signal-to-noise ratio in these data, the lines are consistent with being spectrally unresolved.

Table A.1 shows the measured maser lines toward Cloud C, including archival data. Figure 1 shows the maser spots in position/velocity space.

3.1. Comparison to other H₂CO and SiO maser sources

To provide context, we summarize the other detected SiO and H₂CO masers in the Galaxy. The Sgr B2 maser region, the only other one to have both lines detected as masers, shows a velocity offset between SiO and H₂CO similar to the offset in Cloud C.

Orion KL: The Orion KL SiO masers are well-studied with a long VLBI monitoring program showing that these lines trace the rotating base of an outflow driven by a disk wind (Goddi et al. 2009b; Greenhill et al. 2013). The H₂O and SiO masers are closely matched in velocity and generally spatially close: their emission centroid is on the same position (Greenhill et al. 2013). No H₂CO maser emission is seen toward Orion KL; the H₂CO $1_{1,0} - 1_{1,1}$ emission seen there is thermal with a peak $T_B \approx 40$ K (Mangum et al. 1993).

Sgr B2 (M): There is only one SiO maser spot in Sgr B2, located near Mehringer et al. (1994) H₂CO Source C (not to be confused with Cloud C, the topic of this paper). The Sgr B2 H₂CO maser C is peculiar even among the Sgr B2 masers in that the emission appears to be spatially and spectrally resolved, whereas in other H₂CO masers in Sgr B2, the emission is unresolved. While this might normally hint at thermal emission processes, the high brightness temperature ($T_B \sim 7300$ K) indicates instead that there must be multiple unresolved maser spots within the source. Zapata et al. (2009b) note that the SiO maser is shifted by about 20 km s⁻¹ from the cloud rest velocity,

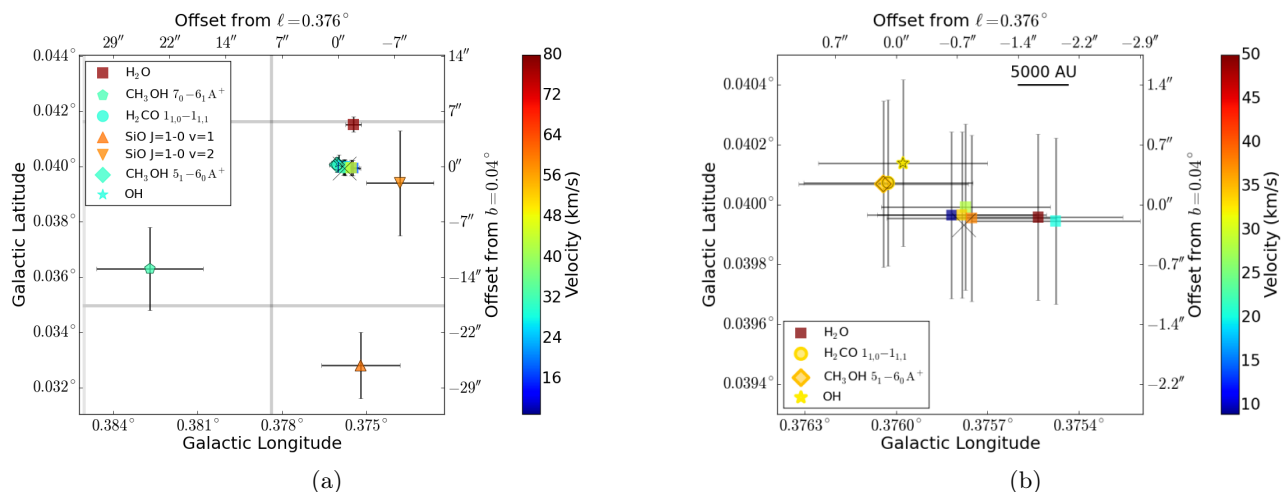


Fig. 1. Overview of the detected masers colored by velocity. The positional errors on the SiO and $\text{CH}_3\text{OH } 7_0-6_1 \text{ A}^+$ measurements are much larger than for the other data sets because the measurements are low signal-to-noise from single-dish observations, yet they are still likely to be underestimated (see Section 3). The gray boxes show the pixel size from the Mopra observations of these lines. (b) is a zoomed-in version of (a) focusing on the interferometer observations. The large X marks the centroid location of the SMA-detected ‘core’ (Walker et al in prep).

$v_{\text{SiO}} = 87 \text{ km s}^{-1}$, while $v_{\text{cloud}} \sim 60 \text{ km s}^{-1}$; by contrast, the H_2CO maser is near the cloud velocity or somewhat blueshifted, with $v_{\text{H}_2\text{CO}} < 55 \text{ km s}^{-1}$ (Mehringer et al. 1994). The remaining Mehringer et al. (1994) H_2CO maser spots do not have corresponding SiO masers.

W51 North: W51 North is a high-mass YSO that exhibits a rich spectrum of NH_3 masers but has no centimeter continuum source (Henkel et al. 2013; Goddi et al. 2015). It is detected in SiO at approximately the cloud rest velocity (Zapata et al. 2009b), but is not detected in $\text{H}_2\text{CO } 1_{1,0}-1_{1,1}$ emission with an upper limit $< 5 \text{ mJy}$ in a 1 km s^{-1} channel (Ginsburg et al in prep).

Other H_2CO sources: The remaining high-mass star-forming regions with H_2CO maser detections in Araya et al. (2007b) and Araya et al. (2008) do not have known corresponding SiO masers (G29.96-0.02, NGC 7538, G23.01-0.41, G25.38-0.18, G23.71-0.20, IRAS 18566+0408). However, of these, only NGC 7538 has been searched for SiO masers (Zapata et al. 2009a). Out of the Araya and Zapata surveys, which each searched ~ 60 sources, there were only 12 sources common to both samples.

4. Discussion

Out of the now eight known H_2CO maser-containing regions in the Galaxy, two are in the CMZ. These two regions, Cloud C and Sgr B2, are the only dense clouds in the CMZ with confirmed ongoing accretion onto a high-mass YSO². Cloud C and Sgr B2 (M) are also the only H_2CO maser

² Sgr C also shows some hints of accretion onto high-mass YSOs via detected outflows (Kendrew et al. 2013) and a 6.67 GHz CH_3OH maser (Caswell et al. 2010), but it has not yet been searched for H_2CO masers. The ultracompact HII regions in Sgr B1 and the 20 and 50 km s^{-1} clouds appear to be more evolved (Mills et al. 2011) and may no longer be accreting. Cloud E contains a compact molecular core and a 6.67 GHz CH_3OH maser (Walker et al in prep, Caswell et al. 2010), but no H_2CO maser is detected. There is one more 6.67 GHz CH_3OH maser source south of G0.253+0.016 that may be an isolated site of high-mass star formation.

sources with corresponding SiO maser detections and vice versa, though the sample of regions explored in both tracers is small.

This high detection rate of masers in star-forming regions within the CMZ, despite limited statistical information, suggests that H_2CO masers may be an efficient tracer of high-mass star formation in extreme environments. By contrast, extensive surveys have shown that the occurrence of H_2CO masers in ‘normal’ high-mass star-forming regions in the Galaxy is very low, $< 2\%$, or 1 of 58 sources in a large survey (Araya et al. 2004, 2007b, 2008; Ginsburg et al. 2011, 2015a).

Given the overall rarity of both SiO masers and H_2CO masers toward star-forming regions and their apparent prevalence in such regions within the CMZ, is there something different about how high-mass star formation proceeds in the CMZ? Physical conditions on parsec scales are known to be very different from those in the disk, with greater turbulent velocity dispersion (Shetty et al. 2012), higher gas temperatures (Ao et al. 2013; Ginsburg et al. 2015b), higher dust temperatures (Battersby et al. in prep), higher pressure (Kruijssen & Longmore 2013), and widespread emission from shock tracers like (thermal) SiO and HNC (Jones et al. 2012). However, maser emission comes from very small regions $\lesssim 100 \text{ AU}$, so why should these parsec-scale differences affect the forming stars?

One possibility is that these rare masers trace a very short period in the lifetime of the forming high-mass YSO. Both masers may trace either an outflow or a disk (Eisner et al. 2002; Goddi et al. 2009a), but the conditions that allow them to maser may in either case last for a very short time. In this scenario, the presence of two such regions in the CMZ indicates that there is currently an ongoing burst of star formation.

Another possibility, which is more closely related to the driving mechanism of the masers, is that high abundance of these species in the CMZ continues from parsec scales down to $\sim 100 \text{ au}$ scales. While H_2CO is abundant throughout the ISM and can be produced in the gas phase, its abundance is greatly increased when grain surfaces are heated

and ices sublimated. SiO is expected to rapidly deplete from gas into dust in the ISM, but its prevalence throughout the CMZ indicates that there is a great deal of dust processing releasing it into the gas phase. CH₃OH is also prevalent throughout the CMZ, and the high abundance required to produce detectable maser emission implies it is formed on icy grain surfaces and subsequently sublimated, so its presence is again an indication of grain destruction or heating. The widespread higher gas-phase abundances of these species may allow all high-mass YSOs to go through a phase of H₂CO and SiO maser emission in the CMZ, while in “normal” Galactic disk star formation, they cannot.

This abundance-based argument would also favor the formation of water masers. However, H₂O masers are underabundant in the CMZ compared to the Galactic disk, though they are present in both Sgr B2 and Cloud C (Walsh et al. 2014). Longmore et al. (2013) note that the ratio of H₂O masers to thermal NH₃ emission is orders of magnitude lower in the CMZ than the rest of the Galaxy. By contrast, there is a (statistically weak) excess of H₂CO and SiO masers. If the H₂O masers come primarily from outflows, it may be that the greater turbulence in the CMZ prevents an adequate path length from being assembled in CMZ gas. Another possibility is that existing H₂O maser observations are not sensitive enough, and a population of lower-luminosity maser sources has so far been missed (Urquhart et al. 2011). Furthermore, the higher pressure and more turbulent CMZ environment means that prestellar cores should form with higher densities (Kruijssen et al. 2014; Rathborne et al. 2014), which may modify which masers are favored.

5. Conclusion

Cloud C in the CMZ dust ridge, a high-mass star-forming region, is revealed as one of the most maser-rich sites in the Galaxy. We have reported new detections of H₂CO 1_{1,0} – 1_{1,1} 4.82966 GHz, CH₃OH 7₀ – 6₁ A⁺ 44.069476 GHz, SiO v=1 J=1-0 43.122079 GHz, and SiO v=2 J=1-0 42.820582 GHz masers. This cloud had not previously been identified as a maser-rich region because both the region and its accompanying masers are faint at all wavelengths compared to neighboring Sgr A and Sgr B2. However, as a maser-rich region, it should prove a useful ground for testing maser mechanisms in unusual masing transitions.

The detection of these masers raises questions about star formation in the CMZ. It is likely that CMZ chemistry and turbulence are different enough from the Galactic disk that masers in the CMZ trace different stages of star formation. Further surveys for rare maser lines toward star forming regions in the inner few hundred parsecs are needed to confirm this speculation. Additionally, further searches for both SiO and H₂CO masers toward a consistent set of target regions would help determine how unique the association between these masers really is.

Acknowledgements. This work made use of MIRIAD (Sault et al. 1995), astropy (Astropy Collaboration et al. 2013), aplypy (aplypy.readthedocs.org), pyspeckit (Ginsburg & Mirocha 2011), ds9 (ds9.si.edu), astroquery (astroquery.readthedocs.org), splatalogue (splatalogue.net) and its member catalogs (Pickett et al. 1998; Müller et al. 2005), and the radio-astro-tools toolkit (radio-astro-tools.github.io). JMDK is funded by a Gliese Fellowship. This letter is based on data from ATCA project C3045.

References

- Ao, Y., Henkel, C., Menten, K. M., et al. 2013, *A&A*, 550, A135
- Araya, E., Hofner, P., & Goss, W. M. 2007a, in *IAU Symposium*, Vol. 242, *IAU Symposium*, ed. J. M. Chapman & W. A. Baan, 110–119
- Araya, E., Hofner, P., Goss, W. M., et al. 2007b, *ApJS*, 170, 152
- Araya, E., Hofner, P., Linz, H., et al. 2004, *ApJS*, 154, 579
- Araya, E. D., Hofner, P., Goss, W. M., et al. 2008, *ApJS*, 178, 330
- Argon, A. L., Reid, M. J., & Menten, K. M. 2000, *ApJS*, 129, 159
- Astropy Collaboration, Robitaille, T. P., Tollerud, E. J., et al. 2013, *A&A*, 558, A33
- Baan, W. A., Guesten, R., & Haschick, A. D. 1986, *ApJ*, 305, 830
- Boland, W. & de Jong, T. 1981, *A&A*, 98, 149
- Caswell, J. L. 1998, *MNRAS*, 297, 215
- Caswell, J. L. 2009, *PASA*, 26, 454
- Caswell, J. L., Fuller, G. A., Green, J. A., et al. 2010, *MNRAS*, 404, 1029
- Chambers, E. T., Yusef-Zadeh, F., & Roberts, D. 2011, *ApJ*, 733, 42
- Deguchi, S., Fujii, T., Glass, I. S., et al. 2004, *PASJ*, 56, 765
- Eisner, J. A., Greenhill, L. J., Herrnstein, J. R., Moran, J. M., & Menten, K. M. 2002, *ApJ*, 569, 334
- Forster, J. R., Goss, W. M., Wilson, T. L., Downes, D., & Dickel, H. R. 1980, *A&A*, 84, L1
- Ginsburg, A., Bally, J., Battersby, C., et al. 2015a, *A&A*, 573, A106
- Ginsburg, A., Darling, J., Battersby, C., Zeiger, B., & Bally, J. 2011, *ApJ*, 736, 149
- Ginsburg, A., Henkel, C., Ao, Y., et al. 2015b [[arXiv:1509.01583v1](https://arxiv.org/abs/1509.01583v1)]
- Ginsburg, A. & Mirocha, J. 2011, *PySpecKit: Python Spectroscopic Toolkit*, *Astrophysics Source Code Library*
- Goddi, C., Greenhill, L. J., Chandler, C. J., et al. 2009a, *ApJ*, 698, 1165
- Goddi, C., Greenhill, L. J., Humphreys, E. M. L., et al. 2009b, *ApJ*, 691, 1254
- Goddi, C., Henkel, C., Zhang, Q., Zapata, L., & Wilson, T. L. 2015, *A&A*, 573, A109
- Greenhill, L. J., Goddi, C., Chandler, C. J., Matthews, L. D., & Humphreys, E. M. L. 2013, *ApJ*, 770, L32
- Henkel, C., Wilson, T. L., Asiri, H., & Mauersberger, R. 2013, *A&A*, 549, A90
- Hoffman, I. M., Goss, W. M., & Palmer, P. 2007, *ApJ*, 654, 971
- Immer, K., Menten, K. M., Schuller, F., & Lis, D. C. 2012, *A&A*, 548, A120
- Jones, P. A., Burton, M. G., Cunningham, M. R., et al. 2012, *MNRAS*, 419, 2961
- Jones, P. A., Burton, M. G., Cunningham, M. R., Tothill, N. F. H., & Walsh, A. J. 2013, *MNRAS*, 433, 221
- Kendrew, S., Ginsburg, A., Johnston, K., et al. 2013, *ApJ*, 775, L50
- Kruijssen, J. M. D., Dale, J. E., & Longmore, S. N. 2015, *MNRAS*, 447, 1059
- Kruijssen, J. M. D. & Longmore, S. N. 2013, *MNRAS*, 435, 2598
- Kruijssen, J. M. D., Longmore, S. N., Elmegreen, B. G., et al. 2014, *MNRAS*, 440, 3370
- Lis, D. C., Li, Y., Dowell, C. D., & Menten, K. M. 1999, in *ESA Special Publication*, Vol. 427, *The Universe as Seen by ISO*, ed. P. Cox & M. Kessler, 627
- Longmore, S. N., Bally, J., Testi, L., et al. 2013, *MNRAS*, 429, 987
- Mangum, J. G., Darling, J., Menten, K. M., & Henkel, C. 2008, *ApJ*, 673, 832
- Mangum, J. G., Wootten, A., & Plambeck, R. L. 1993, *ApJ*, 409, 282
- Mehring, D. M., Goss, W. M., & Palmer, P. 1994, *ApJ*, 434, 237
- Mills, E., Morris, M. R., Lang, C. C., et al. 2011, *ApJ*, 735, 84
- Molinari, S., Bally, J., Noriega-Crespo, A., et al. 2011, *ApJ*, 735, L33
- Müller, H. S. P., Schlöder, F., Stutzki, J., & Winnewisser, G. 2005, *Journal of Molecular Structure*, 742, 215
- Pestalozzi, M. R., Minier, V., & Booth, R. S. 2005, *A&A*, 432, 737
- Pickett, H. M., Poynter, R. L., Cohen, E. A., et al. 1998, *J. Quant. Spec. Radiat. Transf.*, 60, 883
- Pratap, P., Menten, K. M., & Snyder, L. E. 1994, *ApJ*, 430, L129
- Rathborne, J. M., Longmore, S. N., Jackson, J. M., et al. 2014, *ApJ*, 795, L25
- Sault, R. J., Teuben, P. J., & Wright, M. C. H. 1995, in *Astronomical Society of the Pacific Conference Series*, Vol. 77, *Astronomical Data Analysis Software and Systems IV*, ed. R. A. Shaw, H. E. Payne, & J. J. E. Hayes, 433
- Shetty, R., Beaumont, C. N., Burton, M. G., Kelly, B. C., & Klessen, R. S. 2012, *MNRAS*, 425, 720
- Urquhart, J. S., Moore, T. J. T., Hoare, M. G., et al. 2011, *MNRAS*, 410, 1237
- van der Walt, D. J. 2014, *A&A*, 562, A68
- Verheijen, L., Messineo, M., & Menten, K. M. 2012, *A&A*, 541, A36

- Walsh, A. J., Breen, S. L., Britton, T., et al. 2011, MNRAS, 416, 1764
 Walsh, A. J., Purcell, C. R., Longmore, S. N., et al. 2014, MNRAS, 442, 2240
 Whiteoak, J. B., Gardner, F. F., & Pankonin, V. 1983, MNRAS, 202, 11P
 Yusef-Zadeh, F., Hewitt, J. W., Arendt, R. G., et al. 2009, ApJ, 702, 178
 Zapata, L. A., Ho, P. T. P., Schilke, P., et al. 2009a, ApJ, 698, 1422
 Zapata, L. A., Menten, K., Reid, M., & Beuther, H. 2009b, ApJ, 691, 332

-
- ¹ *European Southern Observatory, Karl-Schwarzschild-Strasse 2, D-85748 Garching bei München, Germany*
e-mail: Adam.Ginsburg@eso.org
- ² *International Centre for Radio Astronomy Research, Curtin University, GPO Box U1987, Perth WA 6845, Australia*
- ³ *Max-Planck-Institut für Radioastronomie, Auf dem Hügel 69, D-53121 Bonn, Germany*
- ⁴ *Astron. Dept., King Abdulaziz University, P.O. Box 80203, Jeddah 21589, Saudi Arabia*
- ⁵ *School of Physics, University of New South Wales, Sydney NSW 2052, Australia*
- ⁶ *CSIRO Astronomy and Space Science, P.O. Box 76, Epping, NSW 1710, Australia*
- ⁷ *National Radio Astronomy Observatory, Socorro*
- ⁸ *Astronomisches Rechen-Institut, Zentrum für Astronomie der Universität Heidelberg, Mönchhofstraße 12-14, 69120 Heidelberg, Germany*
- ⁹ *Harvard-Smithsonian Center for Astrophysics, 60 Garden Street, Cambridge, MA 02138, USA*
- ¹⁰ *Leiden Observatory, Leiden University, PO Box 9513, NL-2300 RA Leiden, the Netherlands*
- ¹¹ *Astrophysics Research Institute, Liverpool John Moores University, IC2, Liverpool Science Park, 146 Brownlow Hill, Liverpool L3 5RF, United Kingdom*
- ¹² *Department of Physics and Astronomy and MQ Research Centre in Astronomy, Astrophysics and Astrophotonics, Macquarie University, NSW 2109, Australia*

Appendix A: Spectra & Summary Table

We show the extracted spectra in Figure A.1 and the summary of the detected maser lines in Table A.1.

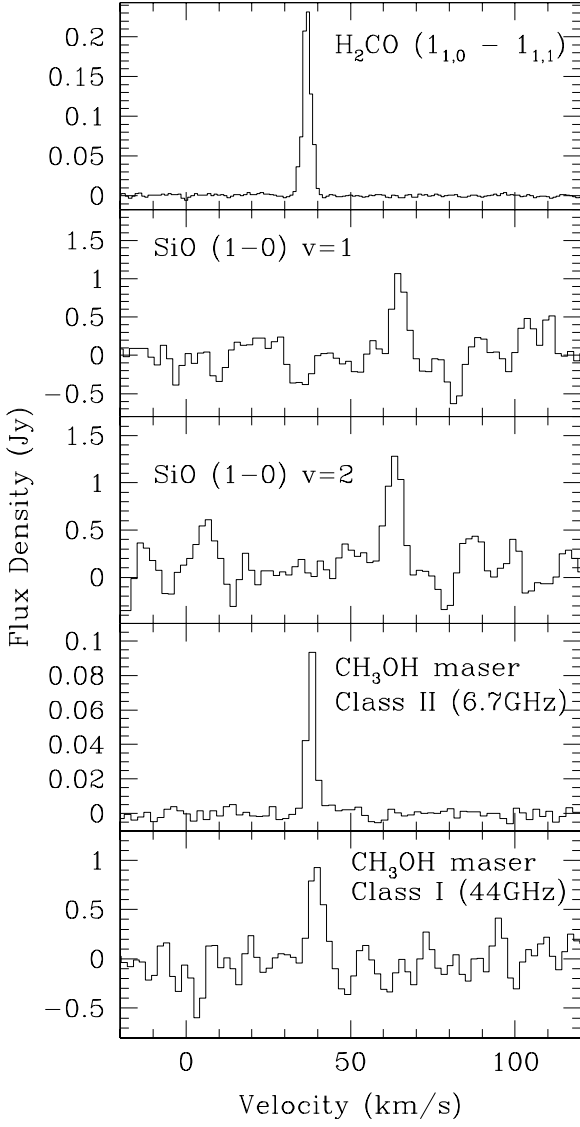


Fig. A.1. Spectra of each of the measured lines. The Mopra data, both SiO lines and the CH₃OH 7₀ – 6₁ A⁺ 44 GHz Class I line, have spectral resolution 3.6 km s⁻¹ and channel spacing 1.8 km s⁻¹. The ATCA data have spectral resolution 1.9 and 1.4 km s⁻¹ and beam shapes 4.85'' × 1.49'' and 9.4'' × 0.46'' for the H₂CO and CH₃OH lines, respectively.

Table A.1. Maser line parameters

Line	ℓ °	b °	$\sigma(\ell)$ ''	$\sigma(b)$ ''	v_{LSR} km s ⁻¹	$\sigma(v_{LSR})$ km s ⁻¹	Measurement
CH ₃ OH 7 ₀ – 6 ₁ A ⁺	0.38270	0.03630	6.8	5.4	39.6	0.4	This Work
H ₂ CO 1 _{1,0} – 1 _{1,1}	0.37603	0.04007	1	1	36.7	0.01	This Work
SiO J=1-0 v=1	0.37520	0.03280	5.04	4.3	64.8	0.4	This Work
SiO J=1-0 v=2	0.37380	0.03940	4.3	6.8	63.2	0.4	This Work
CH ₃ OH 5 ₁ – 6 ₀ A ⁺	0.37604	0.04007	1	1	38.0	0.05	This Work
H ₂ O G000.375+0.042_A	0.37545	0.04153	1	1	78.8	-	Walsh 2014
H ₂ O G000.376+0.040_A	0.37582	0.03996	1	1	9.5	-	Walsh 2014
H ₂ O G000.376+0.040_B	0.37548	0.03995	1	1	24.4	-	Walsh 2014
H ₂ O G000.376+0.040_C	0.37577	0.03999	1	1	32.3	-	Walsh 2014
H ₂ O G000.376+0.040_D	0.37578	0.03997	1	1	37.3	-	Walsh 2014
H ₂ O G000.376+0.040_E	0.37575	0.03995	1	1	40.4	-	Walsh 2014
H ₂ O G000.376+0.040_F	0.37553	0.03996	1	1	52.5	-	Walsh 2014
OH	0.37598	0.04014	1	1	36.0	-	Caswell 1998

Statistical errors on the fit position are given for the single-dish data, and an assumed lower-limit systematic error of 1'' is given for each of the interferometric observations.